SLAC-PUB-8013
November 1998

Possible High Power Limitations From RF Pulsed Heating*

David P. Pritzkau, Gordon B. Bowden, Al Menegat, Robert H. Siemann

Stanford Linear Accelerator Center
Stanford University, California 94309

Abstract. One of the possible limitations to achieving high power in RF structures is damage to metal surfaces due to RF pulsed heating. Such damage may lead to degradation of RF performance. An experiment to study RF pulsed heating on copper has been developed at SLAC. The experiment consists of operating two pillbox cavities in the TE_{011} mode using a 50 MW X-Band klystron. The estimated temperature rise of the surface of copper is 350 °C for a power input of 20 MW to each cavity with a pulse length of 1.5 μs. Preliminary results from an experiment performed earlier are presented. A revised design for continued experiments is also presented along with relevant theory and calculations.

INTRODUCTION

RF pulsed heating occurs due to local Joule heating on a metal surface resulting from a surface magnetic field created from pulsed RF. Ignoring radiation effects, heat deposited on the surface of the metal must flow into the material inducing stress in the lateral dimensions through thermal expansion. Heat flow is governed by the heat diffusion equation, and it is found that the maximum temperature rise occurs at the surface of the metal.

The cyclic stress induced from the application of high pulsed power RF may lead to fatigue of the metal if the stress is large enough to exceed the yield strength of the material. Microcracks formed from fatigue will increase the resistivity of the metal causing Q degradation as well as increased temperature rises. Further cycling will increase the damage and eventually the structure will become unusable.

Due to the short time at which the heat is deposited on the surface of a metal slab, the metal is constrained from lateral expansion. The stress induced from this constraint is related to the temperature rise and a threshold for plastic deformation can be derived (1)

* Work supported by the Department of Energy, contract DE-AC03-76SF00515

Presented at the 4th RF Workshop (RF 98), Pajaro Dunes, Watsonville, California, October 5-9, 1998.

$$\Delta T_y = \frac{(1-\upsilon)Y}{\alpha E} \tag{1}$$

where Y is the yield strength, α is the coefficient of linear expansion, E is Young's modulus and υ is Poisson's ratio. Fatigue cracks are expected to appear for temperature rises of $\Delta T > 2\Delta T_y$ (1). For fully annealed OFE copper this temperature rise corresponds to 40K and for glidcop® 240K. Another source has quoted a safe temperature rise of 110K for copper (2).

The above limits have important consequences for the application of high power RF. In particular, a convenient scaling for RF linear accelerators is (3)

$$\Delta T \propto G^2 \lambda^{1/4} \tag{2}$$

where G is the unloaded gradient and λ is the RF wavelength. Present designs for linear accelerators attempt to achieve higher energies by increasing the gradient. In order to obtain reasonable accelerator lengths and AC power requirements it is necessary to operate at shorter wavelengths (3). If we scale $G \propto \lambda^{-1}$ in accord with the scaling for dark current capture (3) then $\Delta T \propto \lambda^{-1.75}$. Thus smaller wavelengths will result in larger temperature rises. For fixed ΔT one can show that $G \propto \lambda^{-1/8}$. Using parameters from NLC to scale pulsed heating, figure 1 demonstrates that pulsed heating becomes an important impediment to higher gradients at shorter wavelengths as compared to RF breakdown and dark current trapping. The data in figure 1 represent achieved gradient with reasonable dark current (4).

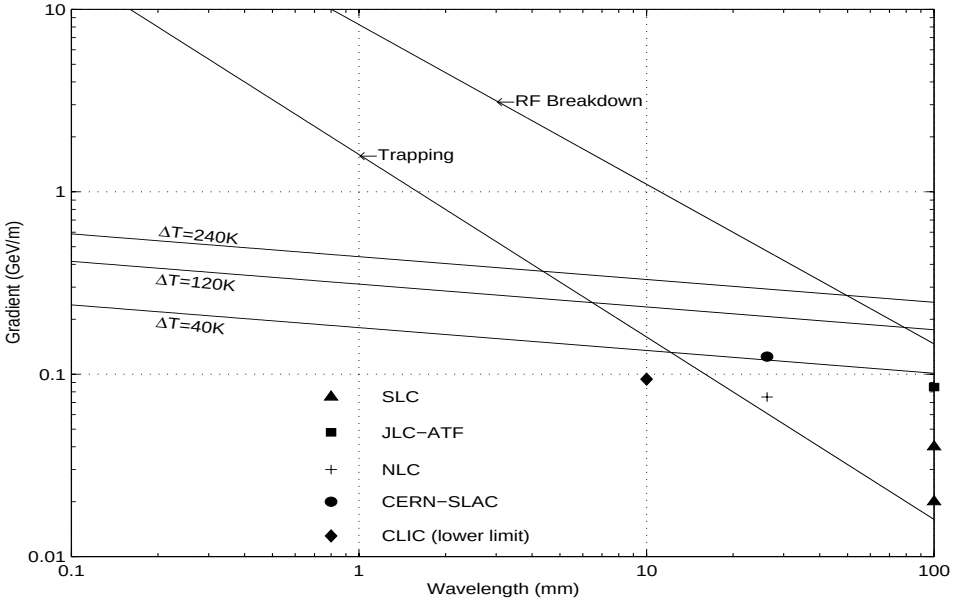

FIGURE 1. Gradient limits due to dark current trapping, RF breakdown, and pulsed heating.

EXPERIMENTAL SETUP

An experiment at SLAC has been created to test for failure of copper due to RF pulsed heating. We define failure as a permanent increase, to within a certain percentage, of the surface resistivity of the metal. Resistivity is an important parameter because it is responsible for determining the unloaded Q of a resonant device as well as the amount of heat the surface of the metal will receive. The lifetime of a material is defined by the number of stress cycles it takes before the material fails. It is known from studies of bulk materials that in general failure is not gradually reached but can happen suddenly after the material has undergone many cycles (5). Of course once this limit is reached, increased degradation will happen quickly. It is also known that in general the number of cycles to failure obeys an exponential dependence on the stress amplitude (6). Higher stresses will result in shorter lifetimes. Hence the experiment will require a relatively high temperature rise in order to feasibly characterize OFE copper and other materials within a reasonable timeframe.

Based on the above scalings of temperature rise with RF wavelength, we opted to create an experiment that utilizes the availability of 50 MW X-Band klystrons at SLAC. The experiment consists of two circularly cylindrical pillbox cavities designed to resonate at 11.424 GHz in the TE_{011} mode. These cavities are connected by an asymmetric magic tee and fed by one klystron. Two cavities are necessary to protect the klystron from reflected power during the RF pulse. A schematic of one such cavity is shown in figures 2 and 3. Accepting losses due to waveguides, we expect a peak input power of 20 MW with a pulse length of 1.5 μs to each cavity at 60 Hz.

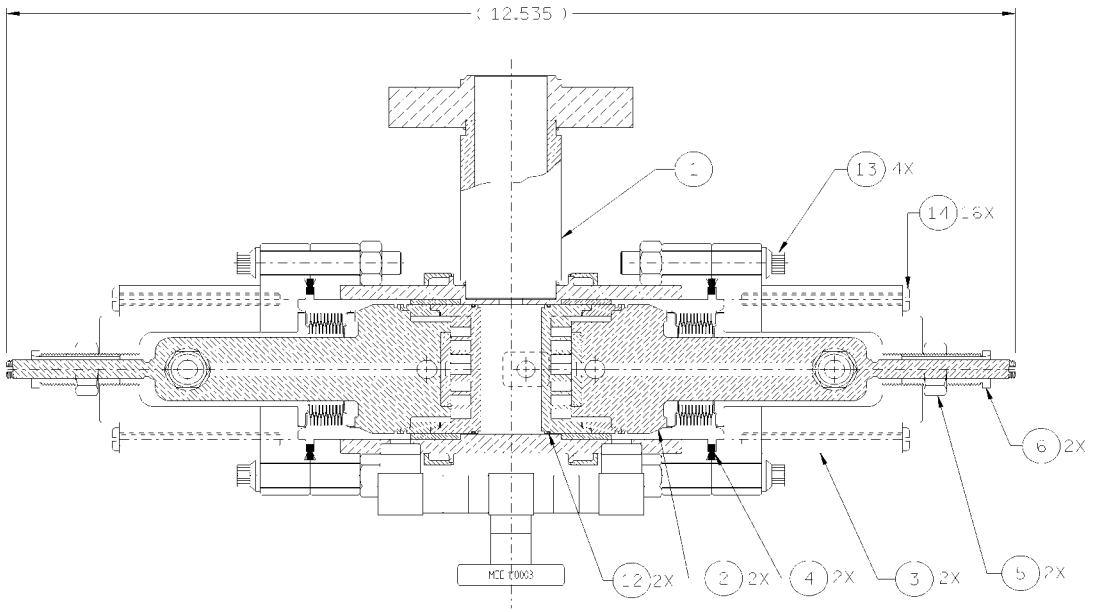

FIGURE 2. Cavity schematic showing main port, vacuum, water-cooling and endcap tuning.

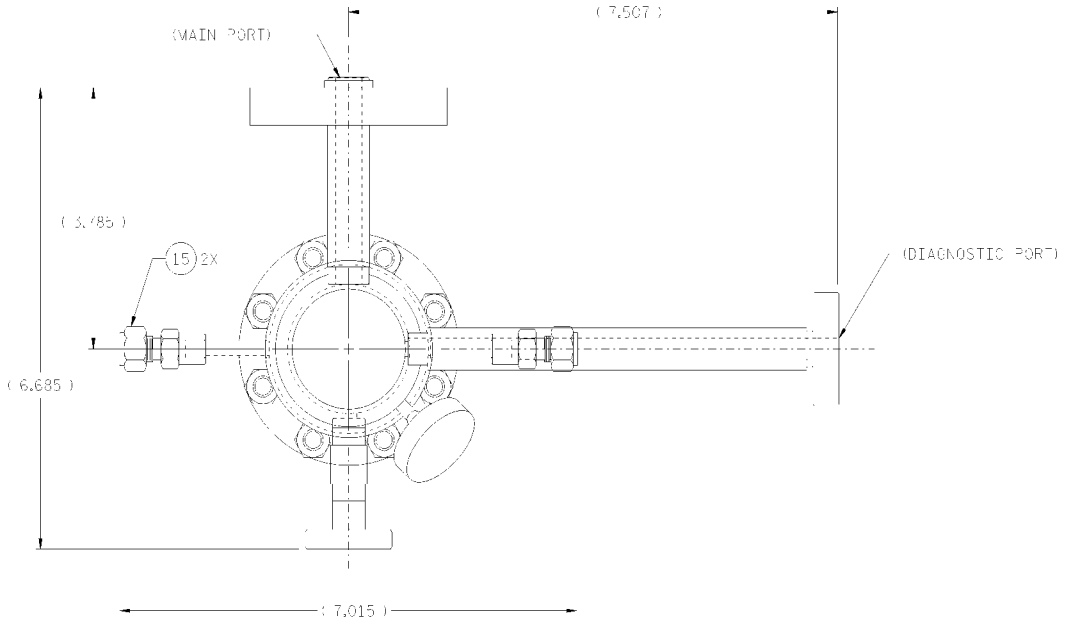

FIGURE 3. Cavity cross-section showing main port, diagnostic port, vacuum and water-cooling.

Cavity Setup

In order to facilitate multiple experiments, the endcaps were designed to be removable. After being machined, the copper endcaps are brazed to stainless steel rings and these assemblies are then welded to stainless steel pistons. After a high-power test is completed, the copper endcaps are removed to conduct further studies. The mating joints on the stainless steel pistons are re-machined and new endcap assemblies are welded on for additional high-power tests. The azimuthal electric fields of the TE_{011} mode allow removable endcaps since electrical contact between the endcaps and the cylindrical wall is not required. Also, figure 2 shows the endcaps attached to bellows that allow mechanical tuning of the cavities.

The cavity body itself cannot be simply replaced, so the dimensions of the cavities were chosen to maximize the heating at the endcaps while minimizing the heating at the cylindrical wall. The cavities have diameters of 4.415 cm and axial lengths of 1.9 cm. The cavity mode is excited through a circular aperture by a WR-90 waveguide operating in the fundamental TE_{10} mode. The coupling is optimized for maximum heating and is found to be β=1.28. The cavity is not critically coupled since the RF pulse length is 1.5 μs and the fill time of the cavity is 0.27 μs.

The degeneracy of the TM_{111} mode is removed by introducing an annular gap of 1.0 mm by 1.0 mm at the outer radius of the endcap (see figure 4). An additional annular gap of 0.1 mm exists between the pistons and the cylindrical wall to allow easy placement and removal of the endcaps into the cavity. A stainless steel spring gasket is used to close this gap with an electrical wall to prevent coaxial modes from

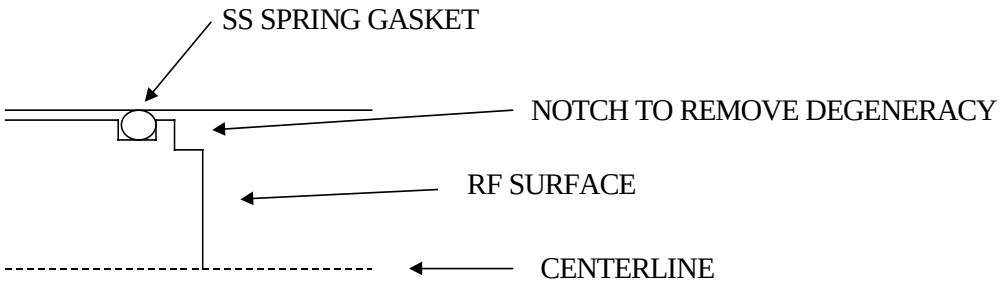

FIGURE 4. Close-up of axisymmetric endcap inside cavity. Schematic is not to scale.

being excited (see figure 4). Using MAFIA (7), it is found that all nearby modes to the TE_{011} mode are at least 100 MHz away and have sufficiently high Q's for the resonant frequency to be outside their bandwidth.

Diagnostic Setup

The local temperature rise of the copper surface will be inferred by measuring the change in the wall Q of the cavity as well as the change of its resonant frequency as a function of time. This measurement will be performed using another port to excite a low power steady-state TE_{012} mode in the cavity at a resonant frequency of 17.811 GHz. This mode is excited through a circular aperture using a waveguide with a width of a WR-42 waveguide and the height of a WR-62 waveguide (see Figure 3). This waveguide is cutoff to 11.424 GHz to prevent high power from leaking out of the cavity. The waveguide is tapered to a full WR-62 after a length of 10 cm in which 11.424 GHz is attenuated by 150 dB. The taper allows the use of available vacuum windows for WR-62 at 17.811 GHz. The diagnostic mode is designed to be critically coupled; however, slide-screw tuners will allow us to vary the coupling if necessary.

The change in wall Q and in the resonant frequency of the diagnostic mode is obtained by measuring the amplitude and phase of the reflected signal from the cavity as a function of time. A schematic diagram of the diagnostic setup is shown in figure 5. The quadrature IF mixer measures the amplitude and phase of the reflected signal. The RF switch is used to measure the cavity Q between pulses to detect when the wall Q becomes permanently degraded. The low-pass filters and the isolators are used to protect the equipment from damage due to RF breakdown and higher harmonics of the klystron frequency. Not shown in figure 5 is the ability to count the number of RF pulses at various power levels used to drive the cavity. A flashADC will digitize the rectangular pulse and an eight-channel event counter will bin the pulse according to its power level.

An RF choke shown in figure 6 is used to prevent the leakage of the 17.811 GHz signal from one cavity to the other. The choke is designed to provide an insertion loss of at least 20 dB for the diagnostic signal while passing the 11.424 GHz signal with

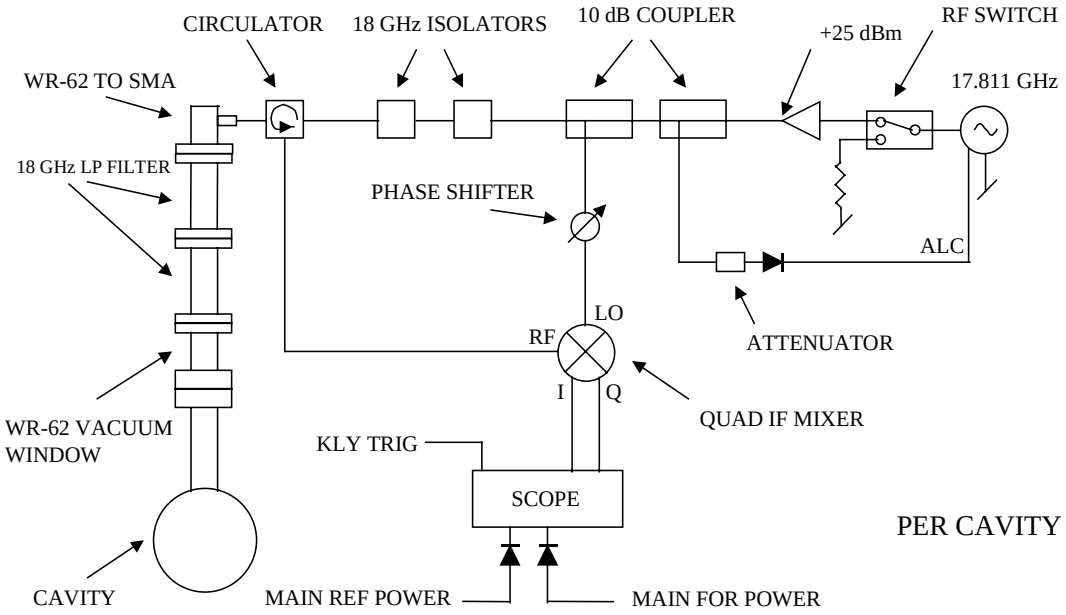

FIGURE 5. Schematic of diagnostic setup.

minimal insertion loss. The width of the choke is tapered from WR-90 to WR-62 to prevent the 17.8 GHz signal from propagating in the TE_{20} mode, while the side-coupled resonators prevent the signal from propagating in the TE_{10} mode.

A third cavity will function as a control for the experiment. It will not receive high power pulses. Before the endcaps are placed into the high-power test cavities, they will be placed into the third cavity and its wall Q will be measured. After the high-power tests are complete, the endcaps will be placed into the third cavity and its wall Q measured once again. This test will isolate the RF properties of the endcaps.

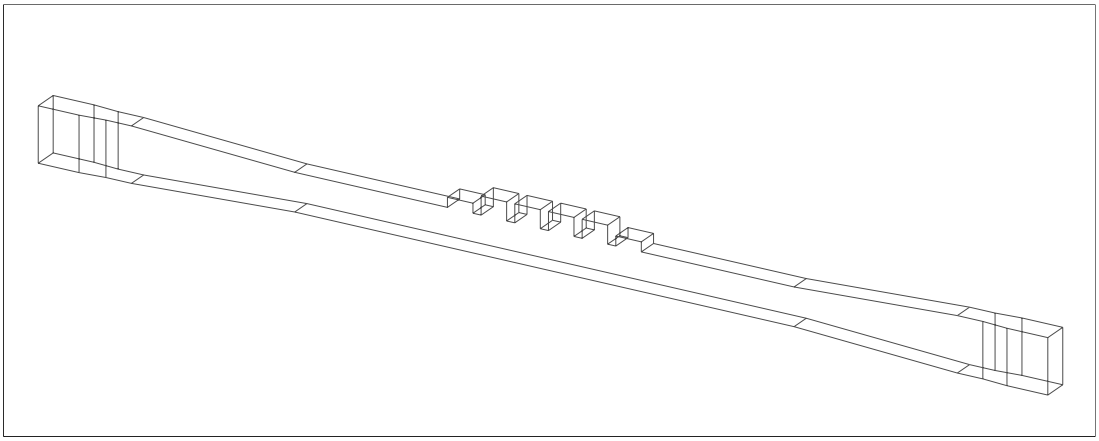

FIGURE 6. Schematic of RF choke. Electric field points out of the paper.

To better characterize the damage to the endcap surfaces after a high-power test, the endcaps were cut with a diamond tool to provide a mirror finish to the surface. Since the same finish cannot be achieved for the surface of the cavity wall, the cavity Q will be determined by two different values of the surface resistivity due to surface roughness. Fortunately, these two values can be uniquely determined from the measurement of the wall Q of both the TE_{011} and the TE_{012} modes.

THEORY

The temperature rise on the copper surface due to pulsed heating is dictated by the well-known heat diffusion equation. Pulsed heating, however, is not to be confused with the steady-state average heating that also occurs in high-power RF structures. The temperature due to average heating can be controlled with water-cooling, but pulsed heating cannot be alleviated in this way.

Although the surface inside the cavity is two-dimensional in nature, for short times each spot on the surface may be approximated as a one-dimensional semi-infinite slab (8). Hence the temperature rise can be found at each point of the surface separately. Since the heat diffusion depth, 13 μm for a 1.5 μs pulse, is an order of magnitude larger than the skin depth at 11.424 GHz, δ=0.62 μm, the skin depth can be ignored in the calculation of temperature rise. We are also only interested in knowing the surface temperature since the maximum temperature rise is found to occur at the surface.

We must include the temperature dependence of the specific heat, thermal conductivity and the resistivity of copper to realistically compute the pulsed temperature rise. For pure copper, this data can be found in references (9) and (10). An integral equation for the temperature rise at the surface of copper is developed

$$\Delta T(\vec{x},t) = \frac{1}{2\sqrt{\pi\rho}} \int_0^t \frac{dt'}{\sqrt{t-t'}} \frac{R_s(\Delta T)\left|H_{\|}(\vec{x},t',\Delta T)\right|^2}{\sqrt{c_\varepsilon(\Delta T)k(\Delta T)}} \tag{3}$$

where $\vec{x}$ is the position along the surface of the cavity, ρ is the density, R_s is the surface resistance, c_ε is the specific heat at constant strain, k is the thermal conductivity and $H_{\|}$ is the surface magnetic field. The specific heat at constant strain is approximated as the specific heat at constant volume. The surface magnetic field is governed by the mode distribution in the cavity as well as a differential equation that models a cavity-waveguide coupled system. The temperature distribution along the surface of the cavity at the end of a pulse is shown in figure 7. The maximum temperature rise occurs along the endcap where the surface magnetic field is at maximum and is predicted to be approximately 350 K. The time evolution of this hot spot is shown in figure 8. Although the temperature rise along the surface of the cylinder wall is greater than the predicted damage threshold from eqn (2), the

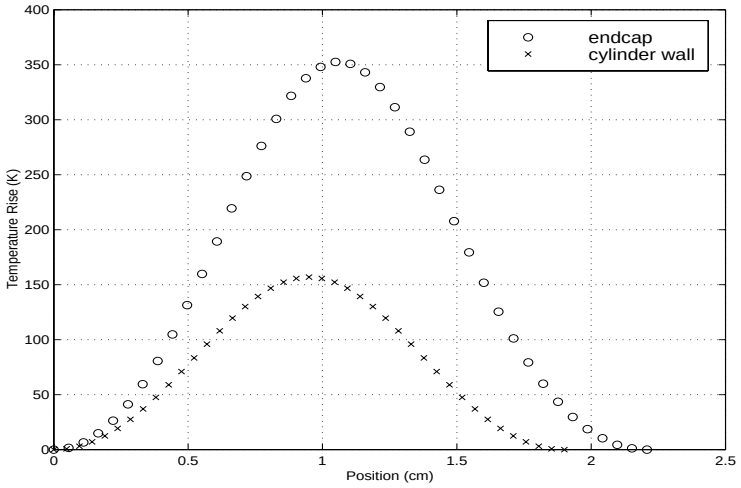

FIGURE 7. Instantaneous temperature rise along the surface of the cavity after a 1.5 μs, 20 MW pulse.

exponential dependence of the number of cycles to failure demonstrates that several high power tests can be conducted before the cavities can no longer be used.

Since the surface resistance will change with temperature, the wall Q of the cavity will also be affected. The predicted change in wall Q for both modes is shown in figure 9. The resonant frequency of the modes will not only shift due to the change in wall Q but also due to the instantaneous thermal expansion of the copper surfaces into the vacuum of the cavity. It is difficult to predict this shift because the induced stresses from pulsed heating are large enough to be beyond the elastic limit. Fortunately, the shift due to the wall Q will oppose the shift due to thermal expansion, and early estimates show that the total shift is about 1/10 of the bandwidth of the diagnostic mode.

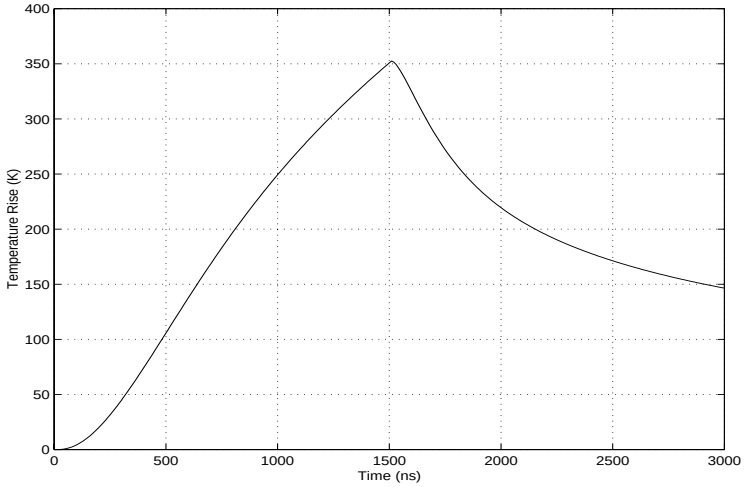

FIGURE 8. The point of maximum temperature rise on endcap for a 1.5 μs, 20 MW pulse.

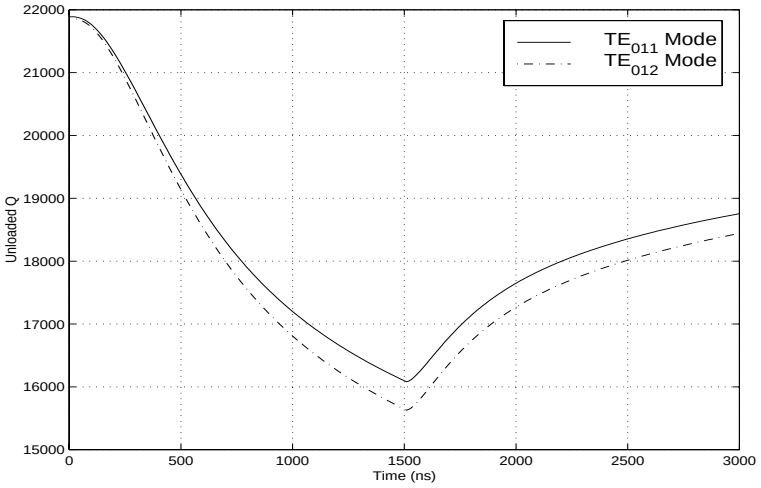

FIGURE 9. Change in wall Q of both modes for a 1.5 μs, 20 MW pulse.

The change in wall Q and in the resonant frequency will cause a change in the amplitude and phase of the reflected signal from the TE_{012} mode. Ignoring effects due to thermal expansion, the predicted reflected power and phase shift as a function of time are shown in figures 10 and 11 respectively. The fill time of the diagnostic mode causes time lags between the peak of the curves and the pulse turn-off.

The model for the cavity-waveguide system is

$$\left(\frac{d^2}{dt^2}+\frac{\omega_\lambda}{Q_L(t)}\frac{d}{dt}+\omega_0^2(t)\right)V_c(t)=\frac{2\omega_\lambda}{Q_e}\frac{dV_f(t)}{dt} \tag{4}$$

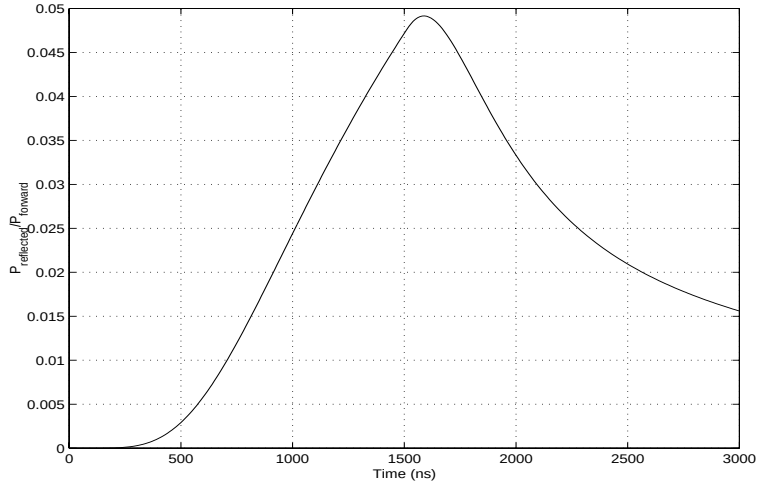

FIGURE 10. Reflected power from the diagnostic mode for a 1.5 μs, 20 MW pulse.

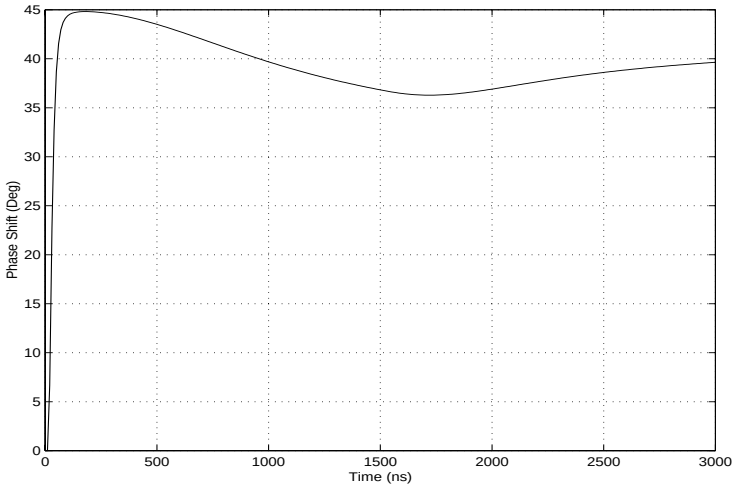

FIGURE 11. Phase shift from the diagnostic mode for a 1.5 μs, 20 MW pulse. Initial phase jump is due to the phase being initially undefined because the mode is critically-coupled.

where ω_λ is the unperturbed angular resonant frequency, ω_0 is the actual angular resonant frequency of the cavity, Q_L is the loaded Q, Q_e is the external Q, V_c is the cavity voltage and V_f is the forward drive voltage. By measuring the amplitude and phase of the reflected voltage as a function of time, $V_r=V_c-V_f$, and substituting back into eqn (4), the change in the loaded Q and in the resonant frequency is determined.

The local temperature rise of the surface may be inferred from the measurement of wall Q by assuming the temperature distribution follows the distribution of the square of the surface magnetic field in the cavity. This method is not completely correct because the surface resistance increases with temperature, so the temperature rise will always be underestimated. Simulations show that the relative error from using this method is on average 5%. This method also requires estimates of the ratio between the maximum temperature rise on the endcap and the maximum temperature rise on the cylinder wall. A lower bound on this ratio is found by assuming the surface resistance remains constant during the heating of the cavity. Fortunately the wall Q for the diagnostic mode is approximately eight times more sensitive to the temperature on the endcap than to the temperature on the cylinder wall, so the relative error involved with this estimate only varies from 1% to 2%.

PRELIMINARY RESULTS

An experiment was performed with an earlier design for the cavity using OFE copper (11); unfortunately, a problem with the design prevented us from reaching an input power of 20 MW to each cavity. RF breakdown occurred in the annular gap between the endcap and the cylinder wall because no means were used to shunt the

gap to prevent coaxial modes. Also, no means were used to prevent the leakage of the 17.811 GHz signal from the cavities which resulted in cross-talk between the two cavities in the experimental setup. Using knowledge of the input power and the coupling to the cavities a conservative estimate of the temperature rise is made. The two cavities in the experiment experienced a temperature rise of at least 100 K for at least 10^7 pulses with no degradation of wall Q. This result does not necessarily imply that a temperature rise of 100 K is safe in terms of RF performance. The result could mean that the lifetime of OFE copper at this temperature rise is longer than 10^7 cycles.

CONCLUSION

The revised design for the cavities will allow pulsed temperature rises that well exceed the range that we expect to see damage to the copper surface. The cavities also allow us the capability of looking at more materials than just OFE copper. One interesting possibility is glidcop whose damage threshold from eqn (2) is ΔT=240 K. Other possibilities may exist to increase the allowed temperature rise such as the use of diamond coating (12). A thin coating of diamond on the copper surface will act as a heat sink since diamond has a higher thermal conductivity than copper. Due to the possible high power limitations of copper, pulsed heating may determine feasible accelerator structures at short wavelengths.

ACKNOWLEDGMENTS

The authors wish to acknowledge Prof. S. Schultz of UCSD for his idea of using a second mode to measure the change in the wall Q of the cavity. The authors also wish to thank E. Colby, R. Dauskardt, X. E. Lin, C.K. Ng, D. Palmer and D. Whittum for many helpful discussions. In addition the authors would like to thank B. Podobedov for his partial translation of (5) from the Russian.

REFERENCES

1. Musal, Jr. H. M., "Thermomechanical Stress Degradation of Metal Mirror Surfaces Under Pulsed Laser Irradiation" in *Laser Induced Damage in Optical Materials 1979*, 1980, p.159.
2. Nezhevenko, O. A., "On The Limitations of Accelerating Gradients in Linear Colliders Due to the Pulse Heating" in *Proceedings of the 1997 Particle Accelerator Conference*, 1998, pp. 3013-3014.
3. Wilson, P. B., "Scaling Linear Colliders to 5 TeV and Above," presented at the ITP Conference on Future High Energy Colliders, University of California, Santa Barbara, California, October 1996.
4. Siemann, R. H., "Advanced Electron Linacs," presented at Symposium on Electron Linear Accelerators, Stanford Linear Accelerator Center, Stanford, California, September 1997.
5. Kovalenko, V. F., *Physics of Heat Transfer and Electrovacuum Devices*, Moscow: Sovetskoe Radio, 1975, ch. 7, p.181.
6. Weroński, A. and Hejwowski, T., *Thermal Fatigue of Metals*, New York: Marcel Dekker, Inc., 1991, ch. 6., p. 164.

7. MAFIA User Guide Version 4.00, CST GmbH, Darmstadt, Germany.
8. Beck, J. V., Cole, K. D., Haji-Sheikh, A., Litkouhi, B., *Heat Conduction Using Green's Functions*, London: Hemisphere Publishing Corporation, 1992, ch. 7, pp. 201-226
9. Lide, D. R., *Handbook of Chemistry and Physics, 77th edition*, New York: CRC Press, 1996, ch. 12, p. 40 and p. 174
10. Furukawa G. T., Douglas, T. B., Pearlman, N., "Heat Capacities" in *American Institute of Physics Handbook, 3rd edition*, New York: McGraw-Hill Book Company, 1972, ch. 4e, p.113
11. Pritzkau, D. P., Menegat, A., Siemann, R. H., Lee, T. G., Yu, D. U. L., "Experimental Study of Pulsed Heating of Electromagnetic Cavities" in *Proceedings of the 1997 Particle Accelerator Conference*, 1998, pp. 3036-3038
12. Lin, X. E., "Diamond Coating in Accelerator Structure", SLAC-PUB-7923, 1998.